Journal of Biomedical Optics

SPIEDigitalLibrary.org/jbo

Nanosurgery of cells and chromosomes using near-infrared twelve-femtosecond laser pulses

Aisada Uchugonova
Matthias Lessel
Sander Nietzsche
Christian Zeitz
Karin Jacobs
Cornelius Lemke
Karsten König

SPIE

Nanosurgery of cells and chromosomes using near-infrared twelve-femtosecond laser pulses

Aisada Uchugonova,[a] Matthias Lessel,[b] Sander Nietzsche,[c] Christian Zeitz,[b] Karin Jacobs,[b] Cornelius Lemke,[d] and Karsten König[a]
[a]Saarland University, Department of Biophotonics and Laser Technology, Campus A5 1, 66123 Saarbruecken, Germany
[b]Saarland University, Experimental Physics, Campus E2 9, 66123 Saarbruecken, Germany
[c]Jena University Hospital, Center of Electron Microscopy, Ziegenmühlenweg, 07743 Jena, Germany
[d]Jena University Hospital, Institute of Anatomy I, Teichgraben 7, 07743 Jena, Germany

Abstract. Laser-assisted surgery based on multiphoton absorption of near-infrared laser light has great potential for high precision surgery at various depths within the cells and tissues. Clinical applications include refractive surgery (fs-LASIK). The non-contact laser method also supports contamination-free cell nanosurgery. In this paper we describe usage of an ultrashort femtosecond laser scanning microscope for sub-100 nm surgery of human cells and metaphase chromosomes. A mode-locked 85 MHz Ti:Sapphire laser with an *M*-shaped ultrabroad band spectrum (maxima: 770 nm/830 nm) and an *in situ* pulse duration at the target ranging from 12 fs up to 3 ps was employed. The effects of laser nanoprocessing in cells and chromosomes have been quantified by atomic force microscopy. These studies demonstrate the potential of extreme ultrashort femtosecond laser pulses at low mean milliwatt powers for sub-100 nm surgery of cells and cellular organelles. [DOI: 10.1117/1.JBO.17.10.101502]

Keywords: ultrashort femtosecond laser; near-infrared; nanosurgery; cells; chromosomes; multiphoton; two-photon imaging.

Paper 11735SSP received Dec. 9, 2011; revised manuscript received Mar. 1, 2012; accepted for publication Mar. 2, 2012; published online May 16, 2012.

1 Introduction

Femtosecond (fs) laser multiphoton technology has gained much attention in biology, biotechnology, and medicine as a promising method for high precision surgery of tissues,[1–7] cells, and intracellular individual organelles,[8–13] including optical injection of molecules, pharmaceutical agents, and genes[14–17] into the cells without any physical contact. When using fs laser microscopes, nanoprocessing as well as non-linear 3D imaging can be performed to visualize the target and to analyze the laser processing effects. Low energy fs pulses allow to realize high localized ultraprecise manipulation of subcellular organelles ranging from several hundred to a few thousand nanometers without causing damage to the manipulated cell itself.

Targeted cellular and subcellular laser manipulations have been used for variety of purposes. Tängenomo et al. used laser microsurgery to find out if Golgi complex is synthesized from a pre-existing template or de novo from endoplasmic reticulum. Golgi apparatus and centriols from living cells were removed by laser dissection. It has been discovered that Golgi biogenesis occurred de novo and in the absence of centrosomes.[18] Choi et al. stimulated cell membrane receptors of astrocytes with the fs laser to generate intracellular calcium waves.[19] Several authors demonstrated the practical usage of fs lasers for individual DNA damage, repair pathways, and mutation studies.[20–22] Fs laser pulses have been used for isolation of single cells of interest from culture, to knock out undesired cells from culture,[23] to stimulate cell growth,[24] to induce cell fusion,[25] embryo enucleation,[26] and neuron cell regeneration.[27] Furthermore, individual mitochondria functionality (cell death, energy production)[28,29] and cellular structures like stress fibers have been studied[30] with the help of fs lasers. Moreover, fs lasers have been used for intracellular delivery of nanoparticles and genes as well as micromolecules into the cells with high efficiency.[14–17] Immediate nuclear gene delivery can be achieved by generating secondary holes on the nuclear membrane in addition to cell membrane perforation.[31]

For the first time König et al. have demonstrated fs laser microscopes for nanoprocessing.[8,9] By definition, the term "nano" is used when dimensions are between 1 and 100 nm. They created structures of less than 100 nm, which is well below the Abbe diffraction limit [near-infrared (NIR) laser wavelength].

Nanocuts within human metaphase chromosomes with a full width of half maximum (FWHM) of 80 nm have been achieved with fs laser pulses as measured by atomic force microscopy (AFM).[9] DNA nanosurgery as precise as 40 nm was realized while using nanoparticles as "light antennas."[12]

Nanoprocessing with near infrared fs laser pulses is based on multiphoton effects at high transient TW/cm^2 light intensities, such as multiphoton ionization and plasma formation. Precise multiphoton nanosurgery requires a short pulse width and a low pulse energy. Two-photon effects and three-photon effects follow a P^2/τ function and a P^3/τ^2 relation, respectively. In multiphoton nanoprocessing, four or more photons are involved in the non-resonant excitation process. Low power levels and pulse energies, respectively, reduce the impact of destructive photodisruptive effects. Uchugonova et al. experimentally demonstrated that cell membrane damage requires about 16 times less energy in the case of 12 fs (5 mW) laser compared to 250 fs (80 mW) laser pulses.[15]

Address all correspondence to: Aisada Uchugonova, Saarland University, Department of Biophotonics and Laser Technology, Campus A5 1, 66123 Saarbruecken, Germany. Tel: +0049 681 302 70456; Fax: 0049 681 302 70452; E-mail: a.uchugonova@blt.uni-saarland.de

0091-3286/2012/$25.00

Here, we used highly focused 85 MHz Ti:sapphire laser pulses in the range of 12 fs to 3 ps for nanosurgery. The aim of the study was to determine at what minimum power (energy) level nanosurgery of human chromosomes and cell nuclei can be performed when using extremely short laser pulses in comparison with longer ones.

2 Material and Methods

2.1 *Femtosecond Laser Microscope*

The fs laser *Integral Pro* 400 oscillator with extremely short pulses of 10 fs (Femtolasers Produktions GmbH, Vienna, Austria) with 0.2 MW peak power, 85 MHz, and $M^2 < 1.3$ was employed. The laser beam was combined with a ZEISS Axio Observer inverted fluorescence microscope equipped with a galvoscanning unit (JenLab GmbH, Jena, Germany) and piezo-driven focussing optics (z stage controller) (nanoMipos400 with digital controller, Piezosysteme Jena). For dispersion pre-compensation of the whole optical system, a set of chirped-mirrors was used. The *in situ* pulse duration was measured by means of a second order interferometric scanning autocorrelator using a non-linear photodiode at the focus of the objective (Femtometer, Femtolasers Production GmbH, Wien, Austria). Typical short pulse duration of 12 fs (*in situ* pulse width) and a bandwidth of about 100 nm, respectively, were measured at the sample plane. This broad spectrum had two maxima (770 and 830 nm) in this particular laser, as measured with a spectrometer. A center wavelength of 800 nm was used for calculations.

The ultracompact scanning microscope with highly-dispersive, large-NA objective (Zeiss EC Plan-Neofluar 40 × / 1.3 oil) was employed. Optionally, double flint glass wedges, and glass blocks have been inserted in the beam path to vary the *in situ* pulse length from 12 fs up to 3 ps. A schematic representation of the setup is demonstrated in Fig. 1.

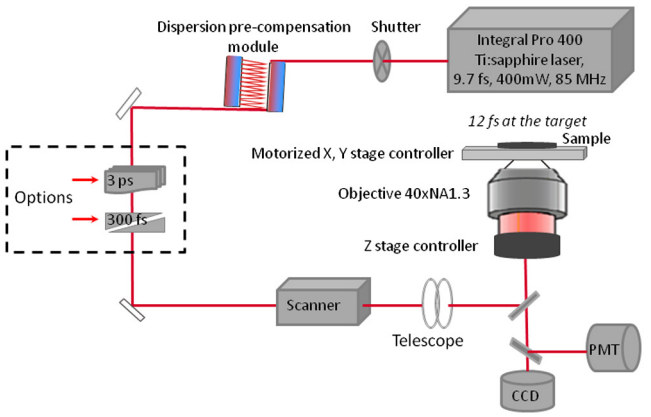

Fig. 1 Schematic representation of the experimental setup. A broadband 85 MHz NIR fs laser was combined with an inverted fluorescence microscope equipped with galvoscanners and piezo-driven focussing optics. An *in situ* pulse width of 12 fs was measured at the sample plane. A dispersion pre-compensation module consisting of chirped mirrors was used to obtain 12 fs laser pulses at the target. Optionally, flint glass wedges and glass blocks have been inserted in the beam path to vary the *in situ* pulse length from 12 fs up to 3 ps. A CCD camera attached to the side port enabled online imaging of the target and the laser beam. A PMT attached to the front port was employed to image two-photon fluorescence.

The microscope was employed in the two-photon fluorescence excitation mode at mean powers in the microwatt range for nondestructive imaging and in the milliwatt range for nanoprocessing in two exposure modes: 1. scanning of a region of interest (ROI) and 2. by single point illumination where the galvoscanners were fixed to a point of interest. A CCD camera attached to the side port enabled online imaging of the target, the laser beam, and the formation of plasma-filled cavitation bubbles. A side-on photomultiplier tube PMT-H7732 (Hamamatsu) with a rise-time of 2.2 ns and a spectral detection range of 185 to 680 nm, according to the producer's data sheet, was employed to detect two-photon fluorescence.

Laser powers were measured with the power meter FieldMaxII-TO™ (Coherent, USA) at the specimen plane. The exposure time was controlled by a shutter controller SC10 (Thorlabs. Inc., New Jersey, USA). Additionally, a motorized stage (Märzhäuzer, Wetzlar) was used to move the samples in x, y directions.

2.2 *Metaphase Chromosomes and Cells*

Metaphase chromosomes were prepared from human peripheral blood cells according to the standard procedure.[32] One group of chromosomes was spread onto cover slips without staining, and the second group was stained with Giemsa and used for photobleaching studies. Other metaphase chromosomes were prepared for high resolution AFM microscopy purposes. Therefore, chromosomes were mounted onto glass cover slides (170 μm thickness) after cleaning with isopropanol/acetone (1 : 1) and coating with 0.01% Poly-L-Lysine (Sigma). Afterward, they were fixed with 2% glytaraldehyde in PBS (phosphate buffer saline) for 10 min, rinsed with distilled water and critical point dried. Figure 2 shows a fluorescent image of human metaphase chromosomes. About 200 μW (12 fs) mean power was required to image chromosome probes fixed with glytaraldehyde. Chromosome probes without staining and stained with Giemsa have been visualized with CCD camera during laser processing.

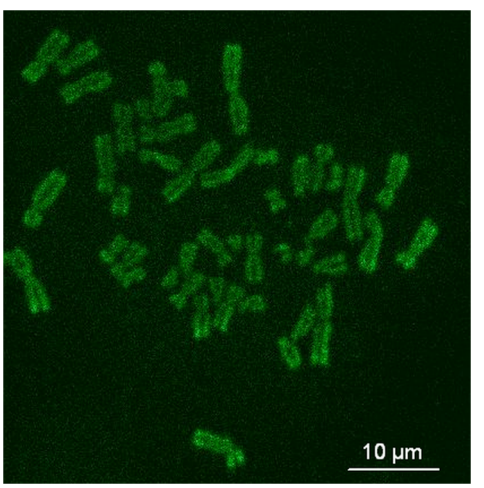

Fig. 2 Metaphase chromosomes of human leukocytes before laser nanoprocessing. The two-photon fluorescence image was taken with a 12 fs (central excitation wavelength at 800 nm, detection filter: BG39) laser pulses at a mean power of 200 μW. The intense fluorescence originates from the fixative 2% glytaraldehyde.

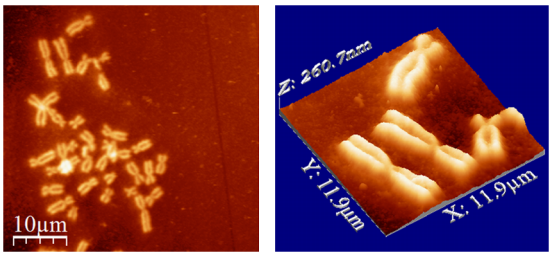

Fig. 3 High resolution 2D and 3D representative topographic AFM images of human metaphase chromosomes. AFM measurements show that the size of metaphase chromosomes varied from 1.6 to 7.0 μm in length. The thickness of two chromatid sisters is between 1.6 and 2.0 μm.

2.3 *Atomic Force Microscope and Image Analysis*

The samples were imaged with a Dimension™ 3100 (Bruker Nano Surface Division, Santa Barbara, CA, USA) AFM in tapping mode (TM). The cantilevers (Micro Cantilever, OMCL-AC160TS-W2, Olympus) with silicon tips at a diameter of about 7 nm, a spring constant of 42 N/m, and a resonance frequency of 300 kHz were used. Images of chromosomes and cells were obtained with different resolutions. Figure 3 shows topographic AFM images of human metaphase chromosomes. As it is shown on the image, the length of human metaphase chromosomes varied from 1.6 to 7.0 μm and the thickness of two chromatid sisters varied from 1.6 to 2.0 μm.

WSxM 4.0 software was used to analyze AFM (.stp) files and measure profiles from line cuts and holes in the cells and chromosomes. AFM images were imported as ASCII matrix (.txt files) format in OriginLab 8G software. The mean cut width was calculated along the whole cut (384 pixels ≡ 24 μm).

3 Results and Discussion

3.1 *Photobleaching Effects of the Laser*

Giemsa stained human chromosomes and cell nuclei on cover slips were used for comparative photobleaching and nano- and microsurgery studies using 12 fs, 300 fs, and 3 ps laser pulses and different mean powers between 0.4 and 5 mW. The laser beam was focused directly into the samples through the cover slip which has a thickness of 170 μm. Cuts were realized by the mode "line scanning." Focused laser beam and bleaching effects of Giemsa were observed with the CCD camera. Typically, a total of 10 s. exposure time was chosen to realize multiple scans per line (12 to 24 ms/scan). Certain distances (500 nm to 2 μm) between lines were realized by means of the motorized stage. Laser processed samples were measured with the AFM microscope to confirm photobleaching and ablation effects on the biological material. Photobleaching effects were observed at powers as low as 0.4 mW (12 fs), 0.8 mW (300 fs), and 1.5 mW (3 ps) (images are not shown). The ablation effects started at higher power levels as confirmed by AFM (Sec. 3.2, Figs. 4 and 5).

3.2 *Nano- and Microprocessing of the Cell Nucleus Dependence on Pulse Width*

To characterize laser ablation effects of laser dependence on pulse width, samples were measured with the AFM microscope in the tapping mode. Interestingly, a very low power of 0.4 mW in the case of 12 fs can already induce visible modifications in the cell nucleus morphology. Due to the non-homogenous structure of the nucleus, the width of the line cuts varied along the line incision. Analysis of each line shows that the width of the line cuts became larger and more homogenous with increased laser powers (Fig. 5). Additionally, slower and longer scan time also resulted in better cuts.

Comparative experiments have been carried out with laser pulses of 12 fs versus 300 fs versus 3 ps. That means the laser pulse width was increased by a factor 25 and 250, respectively. Cells have been cut with different laser mean powers between 0.4 and 5.0 mW at the same conditions. Samples were measured with the AFM, and mean curves have been analyzed. The mean value has been performed over 384 profiles per line. Results show that line cuts can be created with a mean power as low as 0.4 mW ($E = 4.2$ mJ/cm^2, $I_{peak} = 0.35$ TW/cm^2) in the case of 12 fs (Figs. 4 and 5).

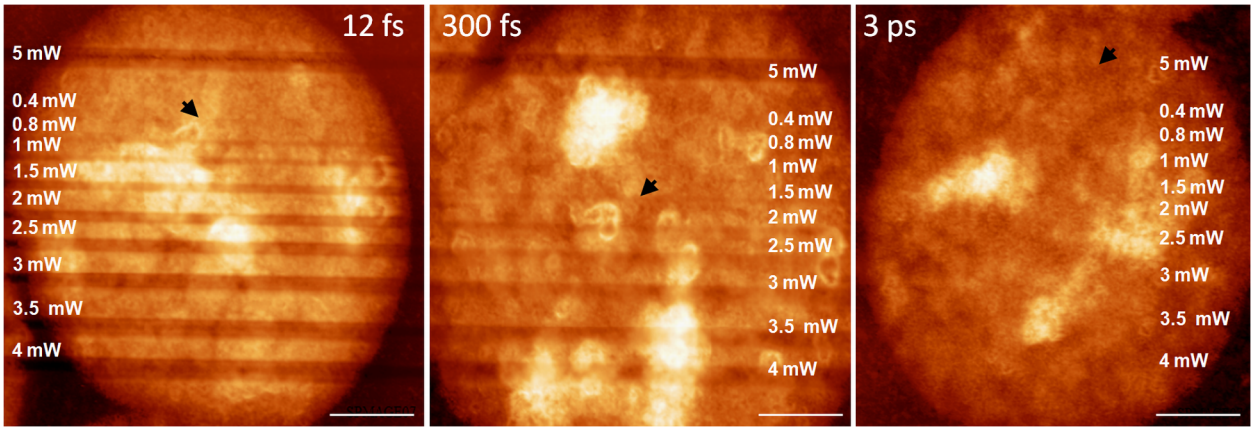

Fig. 4 AFM images of three cell nuclei processed by laser pulses at 12 fs (left) vs 300 fs (middle) and 3 ps (right). The left figure (12 fs) demonstrates that line cuts can be created with a mean power as low as 0.4 mW. In the case of 300 fs, line cuts can be created with 1.5 mW. At 3 ps first ablation effects were seen at 5 mW. Note: AFM images demonstrated laser ablation effects. Photobleaching of Giemsa stained probes was monitored with a CCD camera during laser processing by line scanning with 0.4 to 5 mW mean powers. Photobleaching effects occurred at very low powers of 0.4 mW (12 fs), 0.8 mW (300 fs), and 1.5 mW (3 ps). Total scan time: 10 s. All line scans with 12 fs laser show ablation. Nearly no ablation effects were found in the 3 ps exposed cell nucleus. Scale bar: 4.8 μm.

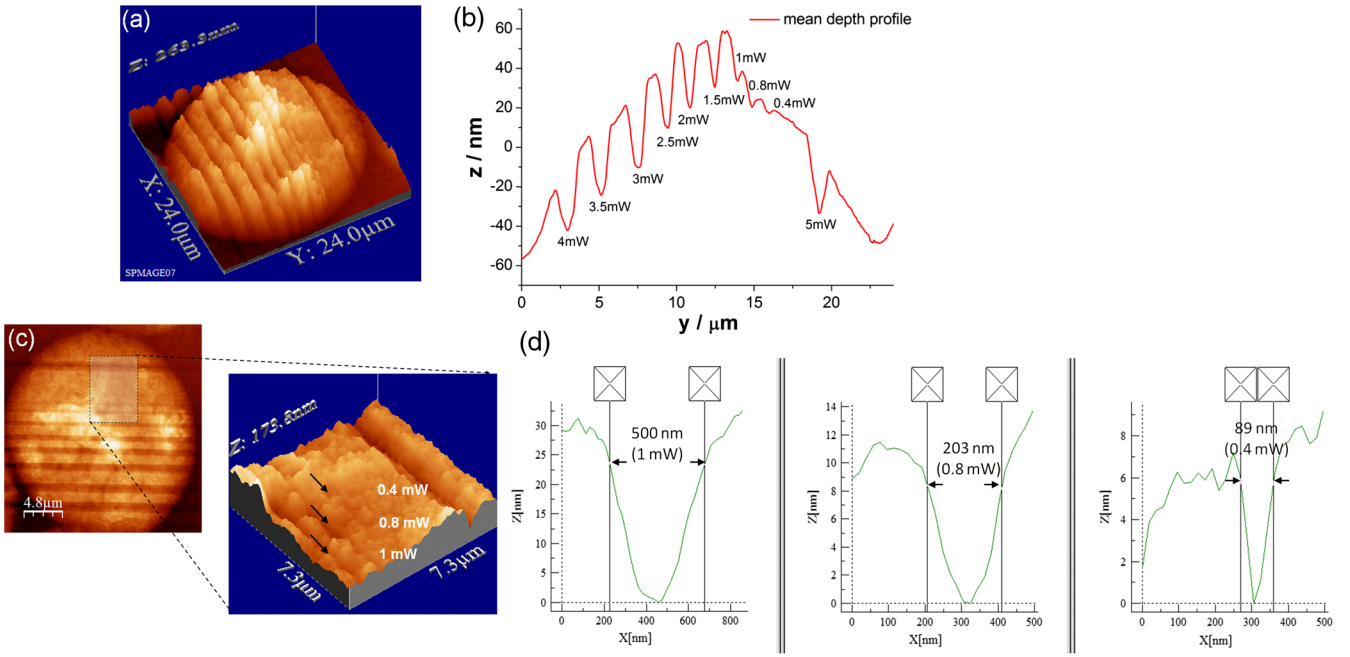

Fig. 5 (a) AFM scans of Line cuts in a cell nucleus realized with 12 fs laser pulses at mean powers (mW) of 4.0, 3.5, 3.0, 2.5, 2.0, 1.5, 1.0, 0.8, 0.4, and 5.0. (b) The graph (mean profile line) indicates that a low laser power of 0.4 mW was sufficient to induce ablation effects. (c) Magnified AFM image with three incisions at 0.4, 0.8, and 1 mW. (d) Analysis of individual line cuts of the cell nucleus shows that sub-100 nm lines can be created with 12 fs laser pulses.

When using 300 fs, ablation effects started at 1.5 mW ($E = 15.9$ mJ/cm^2, $I_{peak} = 0.053$ TW/cm^2). More power P_{th} is required to induce ablation when using picosecond (ps) laser pulses. A value of 5.0 mW ($E = 53.0$ mJ/cm^2, $I_{peak} = 0.017$ TW/cm^2) was determined when using 3 ps. No visible ablation effects were found below 5 mW mean power as demonstrated with the AFM (Fig. 4).

A linear fit with a slope of 0.45 ± 0.03 was determined, when depicting the power values (P_{th}) of 0.4, 1.5, and 5 mW for the onset of ablation versus the pulse length of 12 fs, 300 fs, and 3 ps on a bi-logarithmic scale (Fig. 6). That means that P_{th} is nearly linearly dependent on $\sqrt{\tau}$, which corresponds to a ${P_{th}}^2/\tau$ relation.

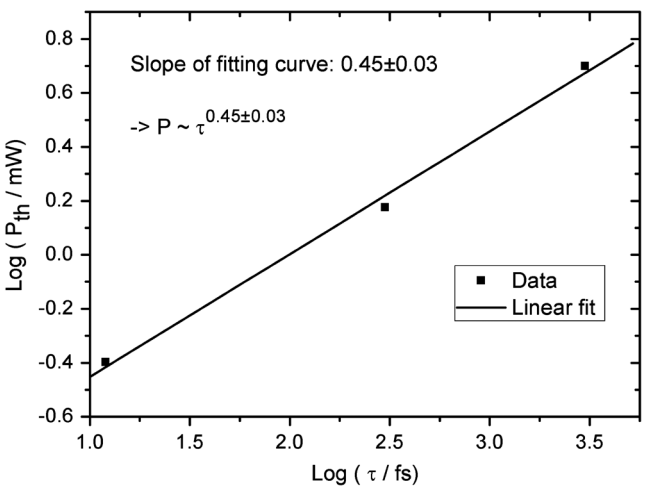

Fig. 6 Threshold powers to induce ablation effects on the cell versus laser pulse width are plotted on a bi-logarithmic scale. The slope of 0.45 ± 0.03 nearly indicates a P^2/τ dependence.

3.3 *Drilling and Cutting Chromosomes with 12 fs Laser Pulses*

Low mean mW powers were sufficient to cut human chromosomes by line scanning and to drill holes by single point illumination (Fig. 7). About 0.7 to 1.0 mW ($E = 7.4$ to 10.6 mJ/cm^2, $I_{peak} = 0.62$ to 0.88 TW/cm^2) laser mean power was sufficient to drill holes into chromosomes with a diameter below 100 nm. Figure 7(b) and 7(c) shows the hole with a diameter of 90 nm and a FWHM of 52 nm created by 12 fs laser. Increased mean powers resulted in bigger holes. Five mW and higher mean powers resulted in disruption of larger parts of the chromosomes.

Experimental results show that the ablation threshold of the laser power depends on fixative or staining dyes, innate components, the density, and the structure of the biomaterials. Non-stained probes require a higher energy than those of stained probes. This corresponds to the findings of König et al.[6] and Kuetemeyer et al.[33] In current study, cutting of metaphase chromosomes required higher intensities/energies than the cutting of the nucleus itself. It may be related to the highly condensed structure of chromosome material of DNA in the chromosomes compared to the nucleus.

However, fs lasers are much more precise than pico- and nanosecond laser pulses because the destructive effects occur after the laser exposure and the major process is multiphoton ionization.[34,35] Photodisruptive effects based on the formation of shock waves and cavitation bubble dynamics can be kept to a minimum. These effects are related to the pulse energy. When using fs laser pulses of low picojoule pulse energies, photodisruptive effects are negligible. There are no plasma shielding effects involved in contrast to nanosecond laser pulses. Detailed explanation on the laser-matter interactions of fs laser pulses versus ps and ns laser pulses was presented by

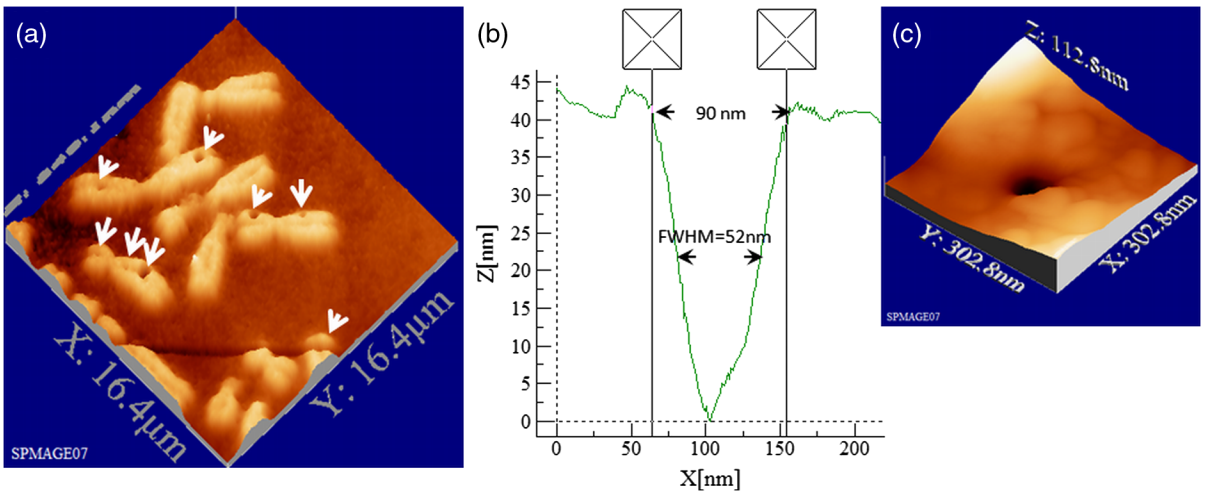

Fig. 7 Topographic AFM images showing cutting and drilling effects of the laser after processing on chromosomes. (a) The arrows show laser produced holes with different diameter size and cut incision. (b) and (c) The measured profile from a hole with a diameter of 90 nm (FWHM of 52 nm).

Vogel et al.[35] They calculated thresholds for laser ablation, which are orders lower for ultrashort pulses versus ns pulses.

The comparative experiments described in this paper with laser pulses of 12 fs versus 300 fs versus 3 ps (laser pulse width increased by a factor 25 and 250, respectively) showed that higher power P_{th} is required for the ablation effect when using ps laser pulses (0.4, 1.5, and 5 mW, respectively).

4 Conclusion

Ultrashort fs lasers have a high value especially in nanobiotechnology, nanomedicine, and cell biology. Nanosurgery/nanomanipulation with fs lasers have been performed for the activation of receptors, delivering of nanoparticles and drugs into the cells, biogenesis and regeneration studies, isolation of subcellular molecules and organelles, etc. Chromosome nanosurgery is one of the interesting applications and can be used to study genetic and cancer diseases, gene mutations, and to perform regeneration studies.

In conventional systems for laser micro- and nanoprocessing, high μJ and mJ pulse energies are employed. However, high pulse energies induce collateral destructive effects. In this paper we demonstrate that extremely short laser pulses at very low pulse energies of some picojoule and sub-milliwatt mean powers, respectively, are sufficient to induce multiphoton ablation effects. We have found that cutting effects with 12 fs pulses resulted in sub-100 nm effects, which are nearly one order lower than the laser wavelength. Destructive effects and the threshold for ablation are dependent upon the structures of biomaterials and chemical substances, such as fixatives. The comparative experiments of 12 fs, 300 fs, and 3 ps laser pulses showed that the ablation effect followed nearly a P^2/τ relation as calculated from the minimum mean powers required to induce morphological changes on biomaterials (0.4 mW at 12 fs, 1.5 mW at 300 fs, 5 mW at 3 ps).

When depicting these ablation threshold power values (P_{th}) of 0.4, 1.5, and 5 mW versus the pulse length of 12 fs, 300 fs, and 3 ps on a bilogarithmic scale, a linear fit with a slope of 0.45 ± 0.03 was determined. That means that P_{th} is nearly linearly dependent on $\sqrt{\tau}$, which corresponds to a ${P_{th}}^2/\tau$ relation.

In summary, sub-100 nm laser surgery can be performed with low mean powers of some hundreds of microwatts up to a few milliwatt. That means, more compact low-price, low-power laser sources could be employed in future in fs laser nanoprocessing and imaging microscopes.

Acknowledgments

The authors wish to thank the German Science Foundation (DFG) for financial support within the program "Schwerpunktprogramm 1327: Optische Erzeugung von sub-100 nm Strukturen für technologische und biomedizinische Applikationen" (Key program: Optical generation of sub-100 nm structures for technical and biomedical applications, project directors: K. König and A. Ostendorf). We are grateful to Dr. Georg Breunig (JenLab GmbH) for kind help with data analysis.

References

1. F. H. Loesel et al., "Non-thermal ablation of neural tissue with femtosecond laser pulses," *Appl. Phys. B: Lasers Opt.* **66**(1), 121–128 (1998).
2. T. Juhast et al., "Corneal refractive surgery with femtosecond lasers," *IEEE J. Sel. Top. Quant. Electron.* **5**(4), 902–910 (1999).
3. U. Tirlapur and K. König, "Near-infrared femtosecond laser pulses as a novel non-invasive means for dye permeation and 3D imaging of localised dye-coupling in the Arabidopsis root meristem," *Plant J.* **20**(3), 363–370 (1999).
4. K. König, "Invited review: multiphoton microscopy in life sciences," *J. Microsc.* **200**(2), 83–104 (2000).
5. K. Koenig, O. Krauss, and I. Riemann, "Intratissue surgery with 80 MHz nanojoule femtosecond laser pulses in the near infrared," *Opt. Express* **10**(3), 171–176 (2002).
6. H. Sun et al., "Femtosecond laser corneal ablation threshold: dependence on tissue depth and laser pulse width," *Laser. Surg. Med.* **39**(8), 654–658 (2007).
7. Y. Liu and M. H. Niemz, "Ablation of femural bone with femtosecond laser pulses—a feasibility study," *Laser Med. Sci.* **22**(3), 171–174 (2007).
8. K. König et al., "Intracellular nanosurgery with near infrared femtosecond laser pulses," *Cell Mol. Biol.* **45**(2), 195–201 (1999).
9. K. König, I. Riemann, and W. Fritzsche, "Nanodissection of human chromosomes with near-infrared femtosecond laser pulses," *Opt. Lett.* **26**(11), 819–821 (2001).
10. W. Watanabe et al., "Femtosecond laser disruption of subcellular organelles in a living cell," *Opt. Express* **12**(18), 4203–4213 (2004).
11. S. H. Chung and E. Mazur, "Femtosecond laser ablation of neurons in *C. elegans* for behavioral studies," *Appl. Phys. A: Mater.* **96**(2), 335–341 (2009).

12. A. Csaki et al., "A parallel approach for subwavelength molecular surgery using gene-specific positioned metal nanoparticles as laser light antennas," *Nano Lett.* **7**(2), 247–53 (2007).
13. L. Sacconi et al., "*In vivo* multiphoton nanosurgery on cortical neurons," *J. Biomed. Opt.* **12**(5), 050502 (2007).
14. U. K. Tirlapur and K. König, "Targeted transfection by femtosecond laser," *Nature* **418**(6895), 290–291 (2002).
15. A. Uchugonova et al., "Targeted transfection of stem cells with sub-20 femtosecond laser pulses," *Opt. Express* **16**(13), 9357–9364 (2008).
16. Z. Foldes-Papp et al., "Trafficking of mature miRNA-122 into the nucleus of live liver cells," *Curr. Pharm. Biotechnol.* **10**(6), 569–78 (2009).
17. S. J. Stevenson, F. Gunn-Moore, and K. Dholakia, "Light forces the pace: optical manipulation for biophotonics," *J. Biomed. Opt.* **15**(4), 041503 (2010).
18. C. Tängemo et al., "A novel laser nanosurgery approach supports de novo Golgi biogenesis in mammalian cells," *J. Cell Sci.* **124**(6), 978–987 (2011).
19. M. Choi et al., "Label-free optical activation of astrocyte *in vivo*," *J. Biomed. Opt.* **16**(7), 075003 (2011).
20. D. Trautlein et al., "Specific local induction of DNA strand breaks by infrared multi-photon absorption," *Nucleic Acids Res.* **38**(3), 1–7 (2010).
21. S. W. Botchway et al., "Use of near infrared femtosecond lasers as sub-micron radiation microbeam for cell DNA damage and repair studies," *Mutat. Res.* **704**(1–3), 38–44 (2010).
22. V. Gomez-Godinez et al., "Analysis of DNA double-strand break response and chromatin structure in mitosis using laser microirradiation," *Nucleic Acids Res.* **38**(22), 1–18 (2010).
23. A. Uchugonova et al., "Optical knock out of stem cells with extremely ultrashort femtosecond laser pulses," *J. Biophoton.* **1**(6), 463–469 (2008).
24. Y.-E. Kuo et al., "Local stimulation of cultured myocyte cells by femtosecond laser-induced stress wave," *Appl. Phys. A: Mater.* **101**(4), 597–600 (2010).
25. K. Kuetemeyer et al., "Femtosecond laser-induced fusion of nonadherent cells and two-cell porcine embryos," *J. Biomed. Opt.* **16**(8), 088001 (2011).
26. K. Kuetemeyer et al., "Combined multiphoton imaging and automated functional enucleation of porcine oocytes using femtosecond laser pulses," *J. Biomed. Opt.* **15**(4), 046006 (2010).
27. A. L. Allegra Mascaro, L. Sacconi, and F. S. Pavone, "Multi-photon nanosurgery in live brain," *Front. Neuroenergetics* **2**(21), 1–8 (2010).
28. N. Shen et al., "Ablation of cytoskeletal filaments and mitochondria in live cells using femtosecond laser nanoscissor," *Mech. Chem. Biosyst.* **2**(1), 17–25 (2005).
29. W. Watanabe et al., "Femtosecond laser disruption of mitochondria in living cells," *Med. Laser Appl.* **20**(3), 185–191 (2005).
30. K. Tanner et al., "Dissecting regional variation in stress fiber mechanics in living cells with laser nanosurgery," *Biophys. J.* **99**(9), 2775–2783 (2010).
31. Y. Hosokawa et al., "Gene delivery process in a single animal cell after femtosecond laser microinjection," *Appl. Surf. Sci.* **255**(24), 9880–9884 (2009).
32. R. S. Verma and A. Babu, *Human Chromosomes. Manual of Basic Techniques*, Pergamon Press, New York (1989).
33. K. Kuetemeyer et al., "Influence of laser parameters and staining on femtosecond laser-based intracellular nanosurgery," *Biomed. Opt. Express* **1**(2), 587–597 (2010).
34. C. L. Arnold et al., "Computational model for nonlinear plasma formation in high NA micromachining of transparent material and biological cells," *Opt. Exp.* **15**(16), 10303–10317 (2007).
35. A. Vogel et al., "Energy balance of optical breakdown in water at nanosecond to femtosecond time scale," *Appl. Phys B: Lasers Opt.* **68**(2), 271–280 (1999).